

# Fractional orbital occupation of spin and charge in artificial atoms

Jordan Kyriakidis\* and Catherine J. Stevenson

*Department of Physics and Atmospheric Science,  
Dalhousie University, Halifax, Nova Scotia, Canada, B3H 3J5*

(Dated: January 28, 2022)

We present results on spin and charge correlations in two-dimensional quantum dots as a function of increasing Coulomb strength (dielectric constant). We look specifically at the orbital occupation of both spin and charge. We find that charge and spin evolve separately, especially at low Coulomb strength. For the charge, we find that a hole develops in the core orbitals at strong Coulomb repulsion, invalidating the common segregation of confined electrons into an inert core and active valence electrons. For excitations, we find a total spin-projection  $S_z = -1/2$  breaks apart into separate occupations of positive and negative spin. This dissociation is caused by spin correlations alone. Quantum fluctuations arising from long-range Coulomb repulsion destroy the spin dissociation and eventually results in all orbitals carrying a negative spin.

PACS numbers: 85.35.Be, 73.21.La, 75.75.+a, 73.21.-b

Quantum dots, especially at zero magnetic field, can often be considered artificial atoms [1, 2]. Like real atoms, artificial atoms can confine a definite number of electrons, and the electronic and magnetic properties are largely governed by the actual number of confined particles. On the other hand, there are dramatic differences between the two which stem primarily and rather obviously from the synthetic nature of quantum dots. Quantum dots are not identical in the quantum-mechanical sense, and they are more tunable [3] than most atomic and condensed matter systems. Both the qualitative and quantitative features of the confinement, for example, are tunable; this, in turn, can be exploited to control the angular-momentum [4] and the spin [5, 6, 7] content of ground and excited states. With respect to the present work, the most significant difference between atoms and electrostatically-defined quantum dots in particular is their size. Due to their much larger size, quantum dots typically have single-particle level spacings of order 1 meV—approximately  $10^4$  times smaller than atoms. Consequently, the relative strength of Coulomb repulsion is also  $10^4$  times larger in quantum dots than it is in atoms. In these quantum dot systems, Coulomb effects are never negligibly small and, for few electron systems especially, the long-range nature of Coulomb repulsion often drives the observed phenomena [8].

Our focus in this work is on the orbital occupation of particles. We seek to determine which orbitals are occupied by charge, which by spin, and how much of each is contained in the given orbitals. We have investigated this question as a function of decreasing dielectric constant, effectively increasing the strength of long-range Coulomb repulsion. We generally find that correlations can be induced both by the spin symmetry as well as Coulomb effects. Spin correlations are most prominent at relatively weak interactions and we find in this regime marked differences between the distribution of charge on the one hand and spin on the other. Coulomb fluctuations gen-

erally destroy this spin-charge distinction, resulting in identical distributions of both spin and charge.

We specifically report here on three main results. First, the common segregation of the charge into an inert core filling the low-lying shells and an active valence shell completely breaks down at strong interactions; the core shells are neither filled nor inert. We find a hole developing in the core as electrons maximise correlations by occupying higher shells, depleting the core. Second, we find that the evolution of the fractional occupation of spin is different than that of charge, making it useful to consider spin and charge as independent entities even though they are both attached to each electron. Thirdly, we look at excitations which preserve the symmetries of the ground state and find significant correlation effects due entirely to the spin symmetry, even in the complete absence of Coulomb effects. We find that a spin excitation of  $S_z = -\hbar/2$  does not merely delocalize across the various orbitals, but rather dissociates into a relatively large negative spin and a small positive spin, such that the global spin symmetry is preserved. Quantum fluctuations due to long-range repulsion destroy this effect and lead to a single delocalized spin with  $S_z = -\hbar/2$ .

Our model is a simple two-dimensional system of  $N$  electrons confined to a circular parabolic potential with long-range Coulomb repulsion. The Hamiltonian is

$$\hat{H} = \frac{1}{2m} \left( \hat{\mathbf{p}} + \frac{e}{c} \mathbf{A} \right)^2 + \frac{1}{2} m \omega_0^2 \hat{\mathbf{r}}^2 + \frac{\alpha}{2\epsilon_{\text{GaAs}}} \sum_{i,j}^{(i \neq j)} \frac{e^2}{|\hat{\mathbf{r}}_i - \hat{\mathbf{r}}_j|}, \quad (1)$$

where the dielectric constant  $\epsilon = \epsilon_{\text{GaAs}}/\alpha$  is scaled by  $\alpha$  relative to that of GaAs ( $\epsilon_{\text{GaAs}} \approx 12.4$ ). Thus,  $\alpha = 0$  describes the non-interacting limit with Coulomb repulsion growing linearly with  $\alpha$ , and with  $\alpha = 1$  describing the GaAs system. Our results below are expressed as functions of  $\alpha$ . In all cases with  $\alpha \neq 0$ , we consider the full long-range ( $\sim 1/r$ ) repulsion.

Our strategy is to first obtain the many-body eigenstates of Eq. (1), including correlation effects. We subsequently analyze these many-body states (rather than just the energies) and directly determine the orbital occupations of the low-lying states.

The numerical approach we adopt is guided by three main requirements. First, we require the full many-body states, properly accounting for all exchange and correlation effects; techniques based on effective single-particle orbitals or those based on obtaining energies only are therefore insufficient. Second, we also require excitations above the the ground state. Indeed we show below that an excitation of a single  $S_z = -1/2$  system results in both positive and negative spin occupation of orbitals. Thirdly, in these confined systems, the strongest correlations often occur for small occupation numbers where appeals to screening effects are invalid.

For these reasons the most appropriate numerical technique is a configuration-interaction (exact diagonalization) approach. This affords the full many-body correlations of the ground state and the excitations, and the few-body systems we consider are not beyond the reach of techniques with a heavy computational load.

The Hamiltonian (1) is exactly solvable in the non-interacting ( $\alpha = 0$ ) limit [9, 10, 11]. In this case, the single-particle eigenstates are a pair of harmonic oscillators  $|nm\rangle$ , whose notation is given in [5]; the quantum number  $n$  is a Landau level index, whereas  $m$  denotes a guiding center. The angular momentum of orbital  $|nm\rangle$  is  $L_z = (n - m)\hbar$  and the energy at zero field of the same orbital is  $E_{mn} = \hbar\omega_0(n + m + 1)$ .

Including spin, then, our single-particle orbitals are denoted by  $|nms\rangle$ . We build the many-body basis states from antisymmetrised tensor products of the single-particle eigenstates,  $|n_1m_1s_1, n_2m_2s_2, \dots\rangle = c_{n_1m_1s_1}^\dagger c_{n_2m_2s_2}^\dagger \dots |\text{vac}\rangle$ .

The various rotational symmetries of Eq. (1) imply conservation of angular momentum projection  $L_z$ , spin projection  $S_z$ , and spin magnitude  $S^2$ . We use these quantum numbers to label the correlated eigenstates of the interacting problem.  $L_z$  and  $S_z$  do not induce correlations, but  $S^2$  may induce correlations. Indeed we show this to be the case particularly for the excitations even in the absence of Coulomb repulsion. In this regime, spin-correlations are strongest.

We denote by  $|S_z, L_z, i\rangle$  the  $i^{\text{th}}$  state  $|n_1m_1s_1, n_2m_2s_2, \dots\rangle$  with fixed angular momentum  $L_z = \sum_k \hbar(n_k - m_k)$  and fixed spin projection  $S_z = \sum_k \hbar s_k/2$  ( $s_k = \pm 1$ ). This state is a single (uncorrelated) antisymmetrised state and is an eigenstate of Eq. (1) in the absence of interactions. Similarly, by  $|S, S_z, L_z, j\rangle$ , we denote the  $j^{\text{th}}$  spin eigenstate with spin magnitude  $\hbar^2 S(S + 1)$ . This state is in general a correlated state

$$|S, S_z, L_z, j\rangle = \sum_i \alpha_i^j |S_z, L_z, i\rangle, \quad (2)$$

whose correlations are due entirely to the spin symmetry. This correlated state is also an eigenstate of Eq. (1)—for  $\alpha = 0$ —and the spectra will generally consist of degenerate subspaces. Finally, the state  $|E, S, S_z, L_z, k\rangle$  denotes the  $k^{\text{th}}$  eigenstate of Eq. (1) with energy  $E$ , and with arbitrary  $\alpha$ . This state contains Coulomb correlations in addition to those imposed by the spin symmetry. It can be written as a coherent superposition of the (correlated) spin eigenstates in Eq. (2):

$$|E, S, S_z, L_z, k\rangle = \sum_j \beta_j^k |S, S_z, L_z, j\rangle. \quad (3)$$

These states will in general lift the degeneracies contained in the spin-correlated states alone.

Our immediate objective is to find all  $E$  and all  $\beta_j^k$  in Eq. (3). In the configuration-interaction method, Eq. (3) can be viewed either as a variational *ansatz* with the  $\beta_j^k$  and the  $E$  as variational parameters, or, equivalently, as a direct matrix diagonalization in the basis of the states  $|S, S_z, L_z, j\rangle$ , where the  $\beta_j^k$  and the  $E$  emerge as the eigenvectors and eigenvalues of the diagonalization procedure. In either case, both views yield identical results and both yield the exact solution in the limit of an infinite number of terms in the sum of Eq. (3).

To construct our many-particle basis states, we start with a sufficiently large set of single-particle orbitals  $|nms\rangle$ . In these calculations, we have taken 288 single-particle states. For a three-particle system with  $S_z = -1/2$ , this gives over  $10^6$  possible three-body states. From these, we consider only those states, Eq. (2), consistent with the desired quantum numbers. These symmetry requirements dramatically reduce the number of basis states and, in practice, we find it rarely necessary to consider greater than  $\sim 10^3$  many-body states  $|S_z, L_z, i\rangle$ . From these states, we form all correlated spin eigenstates  $|S, S_z, L_z, j\rangle$ , Eq. (2), for a given quantum number  $S$ . The  $\alpha_i^j$  can be determined by direct diagonalization of the spin operator  $\hat{S}^2$  in the  $|S_z, L_z, i\rangle$  basis [12]. Alternatively, a closed, analytic, and exact form for the  $\alpha_i^j$  can be determined given the number of singly- and doubly-occupied orbitals using group theory methods and Clebsch-Gordon technology [13, 14].

We use these computed correlated spin states, Eq. (2), as a basis to directly diagonalise the Hamiltonian (1), thus obtaining the coefficients  $\beta_j^k$  in Eq. (3) as well as (less importantly in the present case) the energies  $E$ . A closed form expression for arbitrary many-body matrix elements of the long-range Coulomb interaction exists directly in spectral space [5, 14], obviating the need for real or Fourier space integration.

For a given state  $|\psi\rangle$  of the system, the charge occupation (number of electrons) on the single-particle orbital  $|nm\rangle$  is given by

$$\rho_{\psi}^{nm} = \langle \psi | (c_{nm\uparrow}^\dagger c_{nm\uparrow} + c_{nm\downarrow}^\dagger c_{nm\downarrow}) | \psi \rangle, \quad (4a)$$

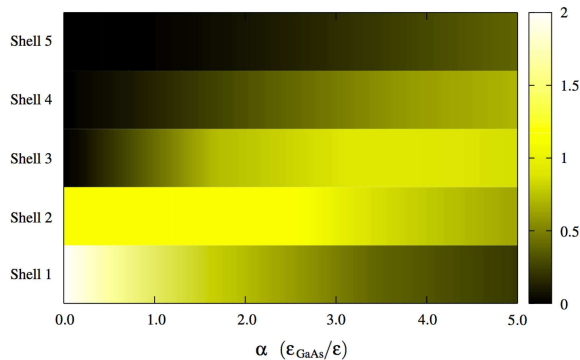


FIG. 1: Fractional orbital occupation of charge in the ground state. The color-scale plot shows how the three particles distribute themselves across the various shells ( $n+m$ ) at different interaction strengths. With increasing interaction strength, a hole develops in the core orbital which, at zero interaction, is doubly occupied. The plot depicts the three-particle ground state at zero field,  $S = 1/2$ ,  $S_z = -1/2$ ,  $L_z = -1$ .

whereas the spin ( $S_z$ ) occupation of the same orbital is

$$S_{\psi}^{nm} = \langle \psi | (c_{nm\uparrow}^{\dagger} c_{nm\uparrow} - c_{nm\downarrow}^{\dagger} c_{nm\downarrow}) | \psi \rangle. \quad (4b)$$

Once the eigenstates have been computed, the expressions in Eq. (4) are evaluated for each orbital ( $m, n$ ).

A three-particle system, at  $B = 0$ , is perhaps the simplest system containing non-trivial spin and charge correlations. Since an odd-number of electrons has finite spin for all states, we can determine how both spin and charge distribute themselves. For weak interactions, the third electron is the sole occupant of the second shell; as Coulomb strength increases, charge correlations can be expected to play an increasingly significant role in the ground state and elementary excitations. A three-particle system, even at fixed orbital occupations [15, 16] may form correlations entirely due to the spin-physics, independent of Coulomb correlations.

At weak fields, the ground state is formed from the manifold of states with definite total spin  $S = 1/2$ , spin projection  $S_z = -1/2$ , and angular momentum  $L_z = -1$  (all in units of  $\hbar$ ).

For the charge degrees of freedom, we have the general sum rule  $\sum_{mn} \rho_{\psi}^{mn} = N$ , where  $N = 3$  is the number of confined electrons. At zero field, the single-particle spectrum consists of degenerate shells, where the  $k$ th shell ( $k = 1, 2, 3, \dots$ ) consists of all orbitals  $|nm\rangle$  satisfying  $n + m = k - 1$ . Figure 1 shows how the particles smear across the shells for various interaction strengths. At zero interactions, the exact ground state is a single anti-symmetrised state of a doubly occupied core (first shell) and a single electron on the second shell [17]. As a function of increasing interaction strength, we find that the distribution broadens. This is expected since the orbital states are no longer eigenstates of the Hamiltonian. Surprisingly, however, the peak of the distribution does not

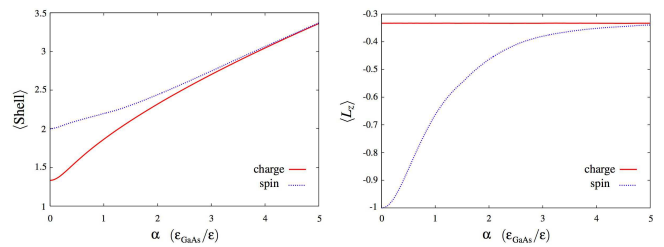


FIG. 2: Separate spin and charge evolution with increasing interaction strength. The panel at left displays the change in the mean shell occupied by spin and charge separately. At right is shown the average angular momentum for both spin and charge. At zero interactions, the spin distribution significantly differs from that of the charge, both among shells and angular momentum. Coulomb-induced fluctuations destroy this order and restore congruence among charge and spin.

remain on the core shell, nor does the occupation of the core drop to unity, thereby allowing exchange to dominate. Instead the core occupation drops below unity, almost to zero, thereby leaving a hole in the core. The electrons gain both exchange and correlation energy by occupying higher shells at the expense of single-particle energy.

In addition to the charge occupation, we can look to the spin occupation. The ground state we are considering here has  $S = 1/2$  and  $S_z = -1/2$ . At zero interactions, the doubly occupied core shell carries no spin; the spin sits in the second shell. Similarly to the charge, this excess spin delocalizes across the orbitals with increasing interaction strength. The evolution of the spin, however, is distinct from that of the charge. In Fig. 2, the distinction is evident. The left panel displays the mean shell occupation for the ground state charge,  $\sum_{m,n} (m+n) \rho_0^{mn}$ , and the ground state spin. Also shown, in the right panel, is the average angular momentum for both spin and charge. For the charge, the *total* angular momentum is set by the global quantum numbers to  $L_z = -\hbar$  and so the average is fixed for all values of  $\alpha$ . These symmetry constraints do not apply to the (excess) spin. Instead, the spin obeys the sum rule  $\sum_{m,n} s_{\psi}^{mn} = -\hbar/2$ .

The distinction between spin and charge distributions is most evident at weak interactions. Here, only spin correlations play a prominent role. Upon increasing Coulomb strength, these additional fluctuations destroy this distinction, resulting in identical mean shell and angular-momentum occupations.

We turn now to excitations above the ground state. In particular, we look at excitations which preserve both angular momentum and spin. We find even stronger correlation effects due entirely to the spin symmetry, independent of the Coulomb correlations. To see this, we look first at the noninteracting limit at zero field, and look at the lowest excitations with the same quantum numbers as the ground state,  $(N, S, S_z, L_z) = (3, 1/2, -1/2, -1)$ .

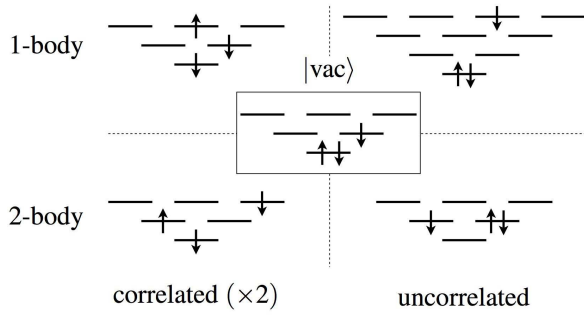


FIG. 3: Spin and angular momentum conserving excitations at zero interactions. At centre is the ground state. The top row depicts one-body excitations and the bottom row two-body excitations. The left column denotes spin correlated states (two per image) while the right denotes spin uncorrelated states.

The lowest-energy excitations lie  $2\hbar\omega_0$  above the ground state, and the subspace is six-fold degenerate. These excitations can be classified by two orthogonal criteria—whether they are a one-body or a two-body excitation, and whether they are a spin correlated or uncorrelated state. The orbital configurations of these degenerate excitations are depicted in Fig. 3. The centre image depicts the ground state (uncorrelated) configuration. The top set of plots shows the two one-body excitations, formed, in this case, by moving a single particle up two shells. (The shell spacing is  $\hbar\omega_0$ .) The bottom set depicts equally energetic configurations, involving an excitation of two particles, each of which moves up a single shell. In contrast, the excitations can also be classified according to their correlations. The two images on the right are uncorrelated states; after antisymmetrization, these states are proper spin doublets ( $S = 1/2$ ). There are no additional degrees of freedom due to spin. The states on the left, however, are not proper spin states even after antisymmetrization. These configurations, containing only singly-occupied orbitals, should be viewed as each representing three states which differ solely by a permutation of the spins. From these three states, two orthogonal  $S = 1/2$  states can be constructed. (The third state has  $S = 3/2$ .) These doublet states are correlated; they cannot be written as a single antisymmetrised (Slater determinant) state in any basis. The correlations, however, are entirely induced by the spin-symmetry requirements and not from Coulomb interactions. (Indeed there are no interactions at  $\alpha = 0$ .)

The implication of correlated excitations is that the excess spin ( $S_z = -1/2$ ) does not sit on a single orbital as in the ground state, even when there is no interaction among the electrons. In fact, it is not even the case that

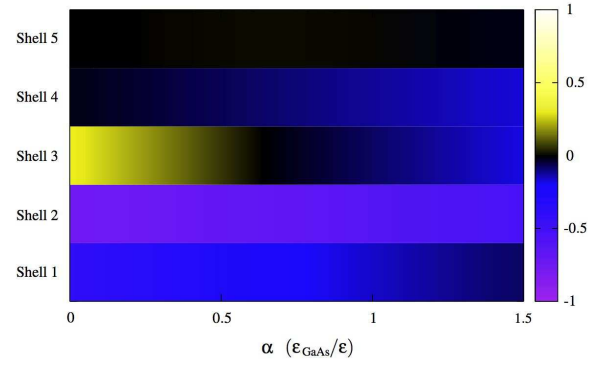


FIG. 4: Spin dissociation at zero interactions and its restoration with Coulomb repulsion. In the presence of only spin correlations ( $\alpha = 0$ ), the spin  $S_z = -1/2$  breaks apart into a small positive component and a larger negative component, each occupying distinct regions of the quantum dot. Coulomb correlations destroy this dissociation, resulting eventually in a single delocalized  $S_z = -1/2$  particle. The color bar is in units of  $\hbar/2$ .

the excess negative spin merely delocalizes. This single negative spin dissociates into a small positive spin and a larger negative spin and these are each distributed on different orbitals. This dissociation can be traced back directly to the correlated doublets in the degenerate manifold. This is shown in Fig. 4, where we plot the net spin ( $S_z$ ) per shell as a function of increasing Coulomb strength. A region of positive spin exists in the third shell while all others have a net negative spin. (The *total* spin is always  $S_z = -\hbar/2$ .) We stress that the dissociation of the spin is not due to Coulomb correlations but is entirely due to the spin correlations. In fact, turning on the Coulomb correlations destroys the effect. This is also shown in Fig. 4; the quantum fluctuations associated with long-range Coulomb repulsion act to destroy the positive spin contribution until all the remaining spin is only of one species.

Correlation effects can be due to either long-range Coulomb repulsion or spin symmetry. At low fields, where low spin is often energetically favoured, spin-correlation effects are strongest and novel spin-induced phenomena may occur. Coulomb fluctuations in general induce different, often much stronger, effects and these charge correlations often overwhelm, destroy, or otherwise mask effects due to the spin symmetry. We have shown here that in the relatively simple and clean system of three interacting electrons with both orbital and spin rotational symmetry the distinction and dissolution of spin-symmetry-induced and Coulomb-induced phenomena can be demonstrated at moderate Coulomb strength.

This work was supported by NSERC of Canada and by the Canadian Foundation of Innovation.

- 
- \* URL: <http://soliton.phys.dal.ca>
- [1] P. L. McEuen, *Science* **278**, 1729 (1997).
  - [2] M. A. Kastner, *Ann. Phys. (Leipzig)* **9**, 885 (2000).
  - [3] L. P. Kouwenhoven, D. G. Austing, and S. Tarucha, *Rep. Prog. Phys.* **64**, 701 (2001).
  - [4] J. Kyriakidis, *J. Phys.: Condens. Matter* **17**, 2715 (2005).
  - [5] J. Kyriakidis, M. Pioro-Ladriere, M. Ciorga, A. S. Sachrajda, and P. Hawrylak, *Phys. Rev. B* **66**, 035320 (2002).
  - [6] A. Kogan, G. Granger, M. A. Kastner, D. Goldhaber-Gordon, and H. Shtrikman, *Phys. Rev. B* **67**, 113309 (2003).
  - [7] J. R. Petta, A. C. Johnson, J. M. Taylor, E. A. Laird, A. Yacoby, M. D. Lukin, C. M. Marcus, M. P. Hanson, and A. C. Gossard, *Science* **309**, 2180 (2005).
  - [8] A. Ghosal, A. D. Güçlü, C. J. Umrigar, D. Ullmo, and H. U. Baranger, *Nature Phys.* **2**, 336 (2006).
  - [9] V. Fock, *Z. Phys.* **47**, 446 (1928).
  - [10] C. G. Darwin, *Math. Proc. Cambridge Phil. Soc.* **27**, 86 (1930).
  - [11] L. Jacak, P. Hawrylak, and A. Wójs, *Quantum Dots* (Springer, Berlin, 1997).
  - [12] A. Wensauer, M. Korkusiński, and P. Hawrylak, *Solid State Commun.* **130**, 115 (2004).
  - [13] T. Helgaker, P. Jørgensen, and J. Olsen, *Molecular Electronic-Structure Theory* (Wiley, Chichester, 2000).
  - [14] M. Rontani, C. Cavazzoni, D. Bellucci, and G. Goldoni, *J. Chem. Phys.* **124**, 124102 (2006).
  - [15] J. Kyriakidis and S. J. Penney, *Phys. Rev. B* **71**, 125332 (2005).
  - [16] J. Kyriakidis and G. Burkard (2006), cond-mat/0606627.
  - [17] There are in fact four degenerate ground states at  $B = 0$ , given by the quantum numbers  $S = 1/2$ ,  $S_z = \pm 1/2$ , and  $L_z = \pm 1$ . Symmetry prevents mixing between these states and the degeneracy is lifted at finite fields. We only consider one of these degenerate states.